Hydration changes upon DNA folding studied by osmotic stress experiments

Shu-ichi Nakano, Daisuke Yamaguchi, Hisae Tateishi-Karimata, Daisuke Miyoshi, and Naoki Sugimoto

Faculty of Frontiers of Innovative Research in Science and Technology (FIRST) and Frontier Institute for Biomolecular Engineering Research (FIBER), Konan University, 7-1-20, Minatojima-minamimachi, Chuo-ku, Kobe, 650-0047, Japan

SUPPLEMENTARY MATERIALS

TABLE S1 Thermodynamic parameters for the hairpin formations of 1a and 1b in the absence and presence of the 20 wt% cosolute[a]

Cosolute	1a			1b		
	$-\Delta G°$ (kcal mol^{-1})	$-\Delta H°$ (kcal mol^{-1})	$-\Delta S°$ (cal mol^{-1}K^{-1})	$-\Delta G°$ (kcal mol^{-1})	$-\Delta H°$ (kcal mol^{-1})	$-\Delta S°$ (cal mol^{-1}K^{-1})
None	1.72±0.01	34.5±3.9	110±14	1.76±0.02	36.8±2.2	113±7
Dex70	1.66±0.01	36.0±0.6	111±2	1.61±0.04	34.2±0.2	105±1
Dex10	1.85±0.02	34.7±0.8	106±3	1.77±0.06	34.7±0.8	106±3
Ficoll	1.68±0.10	34.7±1.6	106±5	1.59±0.03	33.5±1.2	103±4
PEG8000	1.72±0.08	33.0±0.2	105±7	1.76±0.05	34.1±3.0	104±9
PEG200	0.992±0.065	32.5±1.1	102±3	0.937±0.020	33.5±2.8	105±9
EG	1.03±0.05	34.6±1.3	108±4	0.938±0.020	34.1±0.4	107±1
Glyc	1.31±0.05	34.4±1.6	107±5	1.27±0.04	35.9±0.8	112±3
PDO	0.961±0.024	33.5±0.1	104±2	0.899±0.087	33.5±0.4	105±1
MME	0.699±0.070	35.8±3.1	113±10	0.622±0.002	36.4±1.8	115±6
DME	0.582±0.015	41.3±2.4	131±8	0.520±0.044	39.0±0.9	124±3
MeOH	0.717±0.047	36.0±2.3	114±7	0.772±0.053	34.5±2.9	109±9
EtOH	0.550±0.056	34.5±0.2	109±1	0.476±0.010	33.9±4.4	108±15
PrOH	0.167±0.086	32.7±3.6	105±12	0.069±0.039	31.6±5.0	102±16

[a] The values were determined from the curve fit calculation, and the $\Delta G°$ was calculated at 37°C. The error value was determined from the data obtained at the 50 and 2 μM concentrations, except for the data of PEG8000 that was obtained at 10 and 2 μM due to its limited solubility.

TABLE S2 Thermodynamic parameters for the hairpin formations of 2a and 2b in the absence and presence of the 20 wt% cosolute[a]

Cosolute	2a			2b		
	$-\Delta G°$ (kcal mol^{-1})	$-\Delta H°$ (kcal mol^{-1})	$-\Delta S°$ (cal mol^{-1}K^{-1})	$-\Delta G°$ (kcal mol^{-1})	$-\Delta H°$ (kcal mol^{-1})	$-\Delta S°$ (cal mol^{-1}K^{-1})
None	1.87±0.03	35.9±0.01	110±1	1.94±0.09	38.1±1.8	116±6
Dex70	1.87±0.08	40.4±0.8	124±2	1.98±0.08	39.9±1.6	122±5
Dex10	1.91±0.07	35.6±0.1	109±1	1.95±0.07	38.2±0.1	117±1
Ficoll	1.93±0.01	39.6±0.5	121±2	1.95±0.04	41.3±2.6	127±9
PEG8000	1.85±0.04	37.0±0.4	113±1	1.88±0.04	39.3±2.8	121±9
PEG200	1.05±0.08	39.6±0.1	124±1	1.10±0.09	40.4±0.6	127±2
EG	1.17±0.03	40.3±0.2	126±1	1.16±0.01	42.1±1.0	132±3
Glyc	1.39±0.03	38.9±0.1	121±1	1.32±0.03	39.2±1.1	122±3
PDO	1.03±0.05	38.5±2.9	121±9	0.982±0.033	39.1±0.3	123±1
MME	0.562±0.031	39.2±3.0	125±9	0.597±0.041	40.1±1.2	127±4
DME	0.381±0.004	42.5±2.6	136±8	0.358±0.051	40.9±0.7	131±2
MeOH	0.786±0.057	40.0±2.8	126±9	0.783±0.020	42.6±1.4	135±4
EtOH	0.257±0.029	39.0±0.6	125±2	0.221±0.013	42.3±0.4	136±1
PrOH	–0.125±0.034	40.7±0.4	132±1	–0.108±0.094	41.5±2.6	134±8

[a] The values were determined from the curve fit calculation, and the $\Delta G°$ was calculated at 37°C. The error value was determined from the data obtained at the 50 and 2 μM concentrations, except for the data of PEG8000 that was obtained at 10 and 2 μM due to its limited solubility.

TABLE S3 Thermodynamic parameters for the formation of the double-stranded duplexes of the AT-rich 9a and 9b at 0~30 wt% PEG[a]

PEG wt%	**9a**			**9b**		
	$-\Delta G°$ (kcal mol^{-1})	$-\Delta H°$ (kcal mol^{-1})	$-\Delta S°$ (cal mol^{-1}K^{-1})	$-\Delta G°$ (kcal mol^{-1})	$-\Delta H°$ (kcal mol^{-1})	$-\Delta S°$ (cal mol^{-1}K^{-1})
0	5.26±0.22	55.5±2.0	162±3	4.98±0.29	54.6±2.1	160±6
10	4.78±0.33	54.4±2.3	160±7	4.69±0.36	50.9±2.5	149±8
20	4.38±0.20	54.0±1.5	160±4	4.39±0.33	50.6±2.4	149±7
25	4.18±0.19	53.8±1.4	160±4	3.99±0.31	50.2±2.2	149±7
30	3.63±0.25	54.8±1.8	165±6	3.51±0.30	49.1±2.0	147±7

[a] The values were determined from the curve fit calculation and the T_m^{-1} *versus* log (C_t) plot. The $\Delta G°$ was calculated at 37°C. The relatively low duplex stability limited the measurement using PEG up to 30 wt%.

TABLE S4 Thermodynamic parameters for the formation of double-stranded duplexes of the GC-rich 10a and 10b at 0~40 wt% PEG[a]

PEG wt%	**10a**			**10b**		
	$-\Delta G°$ (kcal mol^{-1})	$-\Delta H°$ (kcal mol^{-1})	$-\Delta S°$ (cal mol^{-1}K^{-1})	$-\Delta G°$ (kcal mol^{-1})	$-\Delta H°$ (kcal mol^{-1})	$-\Delta S°$ (cal mol^{-1}K^{-1})
0	12.3±0.4	68.1±3.0	180±9	11.7±0.1	67.5±1.1	180±3
10	11.7±0.2	67.2±1.7	179±5	11.1±0.2	65.7±1.5	176±4
20	11.1±0.4	64.4±3.2	172±10	10.3±0.3	65.5±2.4	178±7
30	9.96±0.62	63.0±4.8	171±13	9.41±0.42	64.0±3.0	176±9
40	8.68±0.30	61.1±2.2	169±7	8.36±0.18	61.4±1.3	171±4

[a] The values were determined from the curve fit calculation and the T_m^{-1} *versus* log (C_t) plot. The $\Delta G°$ was calculated at 37°C.

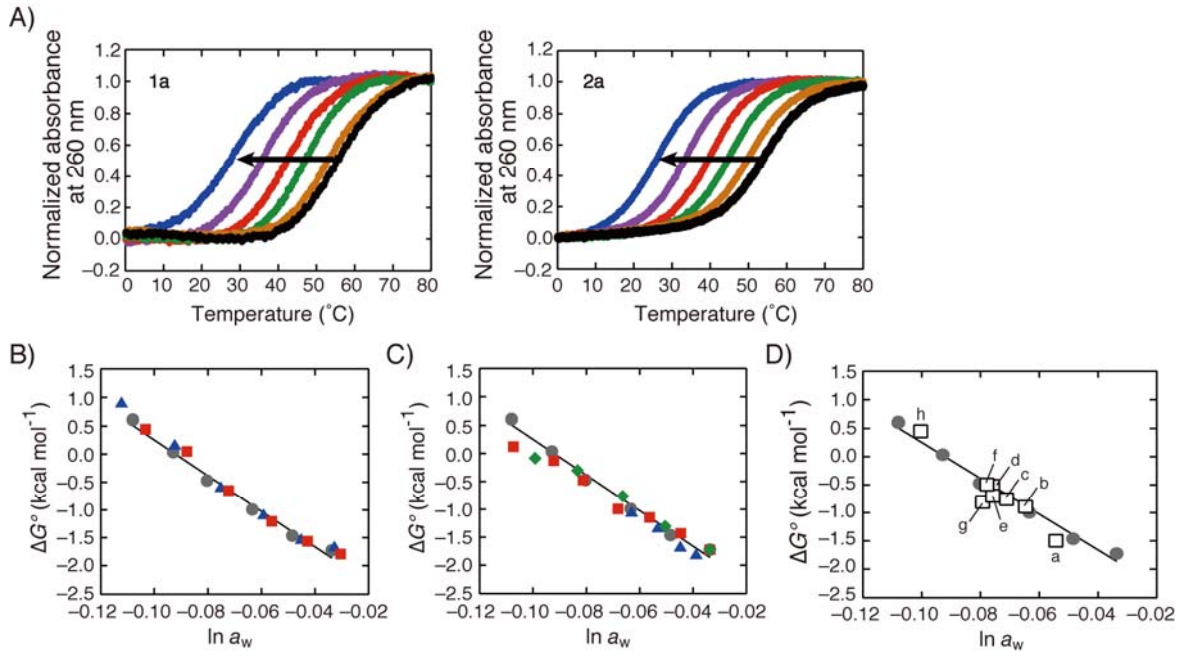

FIGURE S1. (A) UV melting curves of **1a** (left) and **2a** (right) at 2 μM concentration in the absence and presence of PEG200. The melting temperatures are 54.3, 53.1, 47.2, 42.6, 35.9, and 30.0 °C for **1a** and 54.7, 50.6, 46.6, 40.2, 34.0, and 27.0°C for **2a** when increasing the amount of PEG from 0 to 50 wt%, indicated by arrow. (B) The plots for **1a** against the logarithm of the water activity, obtained using the PEG200 solutions containing NaCl (circles), KCl (triangles) or CsCl (squares) at 1 M. (C) The plots for **1a** against the logarithm of the water activity, obtained using the 1 M NaCl solutions of 10~50 wt% PEG200 (circles), 5~20 wt% PEG8000 (triangles), 5~30 wt% dimethoxyethane (squares), or 5~20 wt% 1-propanol (diamonds). (D) The plots for **1a** obtained using the binary mixture solutions of (a) 10 % PEG200/10 % PEG8000, (b) 10 % PEG200/10 % DME, (c) 1 M DME/1 M PrOH, (d) 10 % PEG200/10 % PrOH, (e) 1 M PEG200/1 M DME, (f) 1 M PEG200/1 M PrOH, (g) 20 % PEG200/20 % PEG8000, and (h) 20 wt% PEG200/20 wt% DME, in comparison to the data of 0~50 wt% PEG200 (circles).

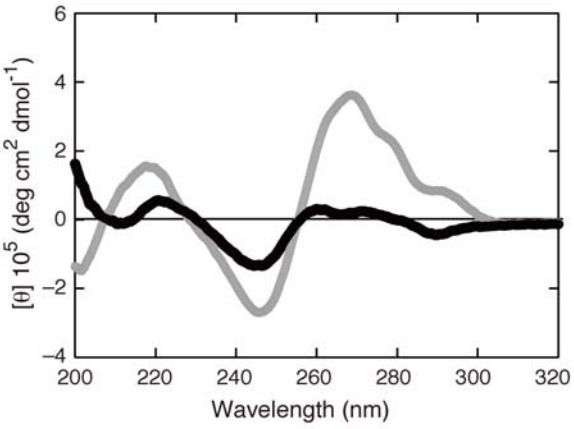

FIGURE S2. Circular dichroism (CD) spectra of the DNA duplexes containing the 5′-pyrimidine-GA-purine-3′ (gray) and 5′-purine-GA-pyrimidine-3′ sequences (black) shown in Fig. 2C. The spectra were measured with 40 μM in the 1 M NaCl-phosphate buffer.

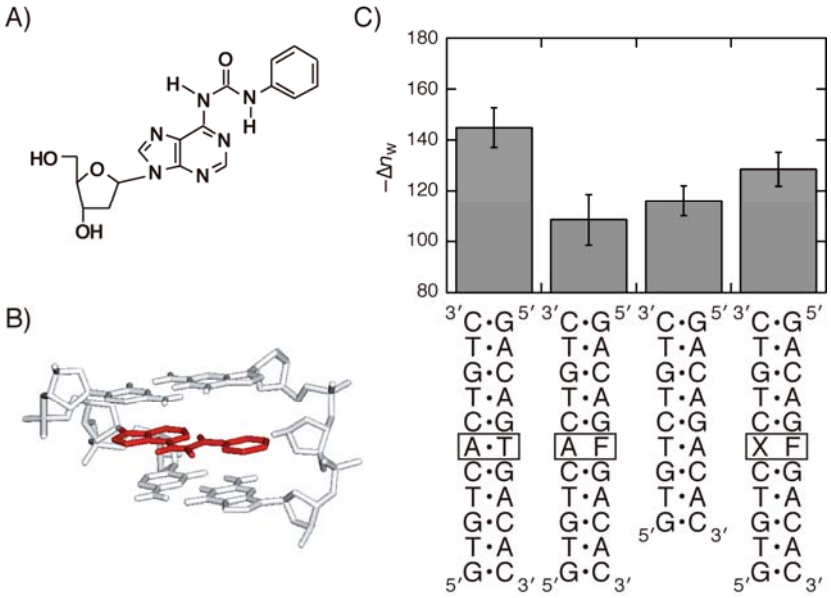

FIGURE S3. (A) Structure of A^{phe} (*N*6-(*N*′-phenylcarbamoyl)-2′-deoxyadenosine) as an A/T base-pair analog. (B) The stacking model of A^{phe} (colored in red) opposite the tetrahydrofuran abasic site in a DNA duplex. (C) The values of Δn_w for the 11-mer duplexes having different base pairs in the middle and that for the 9-mer duplex without the trinucleotide interactions in the middle of the 11-mer duplex. F and X indicate the tetrahydrofuran abasic site and A^{phe}, respectively.

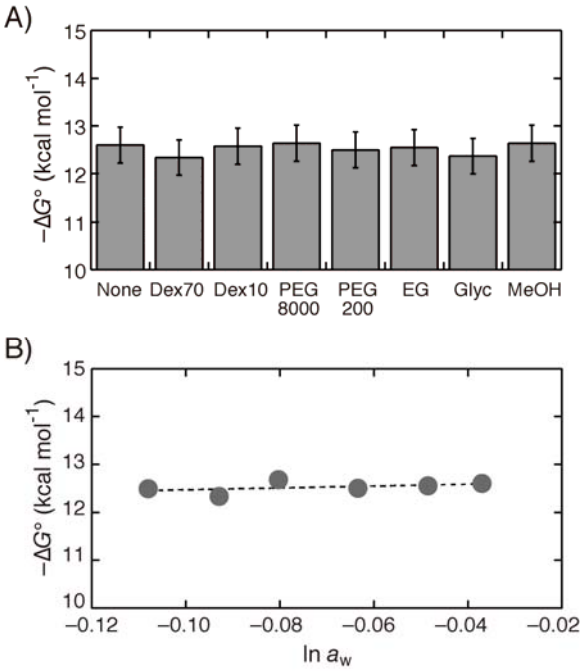

FIGURE S4. (A) The self-complementary PNA sequence and the plot of $\Delta G°$ *versus* ln a_w for the PNA duplex. (B) The $\Delta G°$ of the duplex formed by the self-complementary PNA sequence ^{N}ATGCGCAT^{C} obtained in various solutions containing cosolutes at 20 wt%.

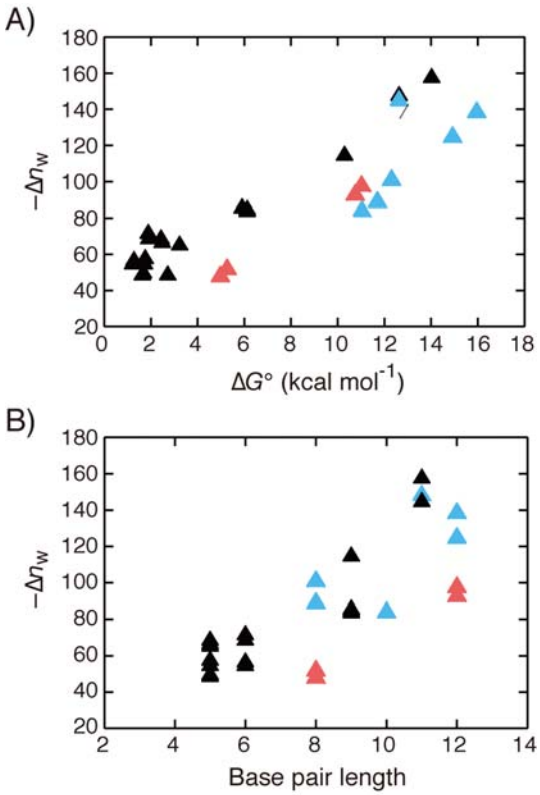

FIGURE S5. (A) The plot of $-\Delta n_w$ *versus* the thermodynamic stability and (B) the plot of $-\Delta n_w$ *versus* the length of the Watson-Crick base pairs of the oligonucleotide duplexes examined in this study. The colored symbols represent the data for biased sequences of continuous A/T (red) or G/C base pairs (blue) longer than 4.